An isotopic view on the connection between photolytic emissions of NO x from the Arctic snowpack and its oxidation by reactive halogens

S. Morin, J. Erbland, Joel Savarino, F. Domine, J. Bock, U. Friess, H.-w. Jacobi, H. Sihler, J. Martins

An isotopic view on the connection between photolytic emissions of NO_x from the Arctic snowpack and its oxidation by reactive halogens

S. Morin,[1] J. Erbland,[2] J. Savarino,[2] F. Domine,[2,3] J. Bock,[2] U. Friess,[4] H.-W. Jacobi,[2] H. Sihler,[4,5] and J. M. F. Martins[6]

Received 26 July 2011; revised 15 November 2011; accepted 16 November 2011; published 21 January 2012.

[1] We report on dual isotopic analyses ($\delta^{15}N$ and $\Delta^{17}O$) of atmospheric nitrate at daily time-resolution during the OASIS intensive field campaign at Barrow, Alaska, in March–April 2009. Such measurements allow for the examination of the coupling between snowpack emissions of nitrogen oxides (NO_x = NO + NO_2) and their involvement in reactive halogen-mediated chemical reactions in the Arctic atmosphere. The measurements reveal that during the spring, low $\delta^{15}N$ values in atmospheric nitrate, indicative of snowpack emissions of NO_x, are almost systematically associated with local oxidation of NO_x by reactive halogens such as BrO, as indicated by ^{17}O-excess measurements ($\Delta^{17}O$). The high time-resolution data from the intensive field campaign were complemented by weekly aerosol sampling between April 2009 and February 2010. The dual isotopic composition of nitrate ($\delta^{15}N$ and $\Delta^{17}O$) obtained throughout this nearly full seasonal cycle is presented and compared to other seasonal-scale measurements carried out in the Arctic and in non-polar locations. In particular, the data allow for the investigation of the seasonal variations of reactive halogen chemistry and photochemical snowpack NO_x emissions in the Arctic. In addition to the well characterized peak of snowpack NO_x emissions during springtime in the Arctic (April to May), the data reveal that photochemical NO_x emissions from the snowpack may also occur in other seasons as long as snow is present and there is sufficient UV radiation reaching the Earth's surface.

Citation: Morin, S., J. Erbland, J. Savarino, F. Domine, J. Bock, U. Friess, H.-W. Jacobi, H. Sihler, and J. M. F. Martins (2012), An isotopic view on the connection between photolytic emissions of NO_x from the Arctic snowpack and its oxidation by reactive halogens, *J. Geophys. Res.*, *117*, D00R08, doi:10.1029/2011JD016618.

1. Introduction

[2] The discovery of naturally occurring ozone depletion events in the early 1980s in the Arctic lower troposphere during springtime [*Bottenheim et al.*, 1986] has triggered in-depth investigations into atmospheric chemical processes occurring in the polar boundary layer [*Dominé and Shepson*, 2002; *Simpson et al.*, 2007; *Grannas et al.*, 2007]. The combination of field, laboratory and modeling studies have unveiled several key processes occurring in the Arctic and Antarctic lower atmosphere in springtime, such as: (1) reactive halogen-catalyzed ozone destruction in the marine boundary layer (MBL), through the so-called "bromine-explosion" mechanism [*Barrie et al.*, 1988; *Hausmann and Platt*, 1994; *Simpson et al.*, 2007]; (2) UV-induced photolysis of trace species deposited in the snowpack leading to the emission of reactive species such as nitrogen oxide (NO_x = NO + NO_2), nitrous acid (HONO) or formaldehyde (HCHO) into the atmosphere [*Honrath et al.*, 1999; *Sumner and Shepson*, 1999; *Zhou et al.*, 2001; *Grannas et al.*, 2007]; and (3) oxidation of gaseous elemental mercury and its subsequent deposition to the surface [*Schroeder et al.*, 1998; *Steffen et al.*, 2008]. The degree of knowledge of the cross-interactions between these three classes of processes is variable. For instance, the link between halogen-induced ozone destruction and mercury deposition events was soon realized [*Schroeder et al.*, 1998; *Lu et al.*, 2001; *Steffen et al.*, 2008; *Dommergue et al.*, 2010]. The impact of photochemical reactions occurring within the snowpack on the overlying atmosphere was recognized, mostly in terms of local sources of OH radicals in the lower atmosphere, originating from the atmospheric photolysis of snowpack-emitted precursors such as HONO and HCHO [*Sumner and Shepson*, 1999; *Zhou et al.*, 2001; *Dominé and Shepson*, 2002; *Grannas et al.*, 2007]. The impact of NO_x

[1]Météo-France – CNRS, CNRM-GAME URA 1357, CEN, Grenoble, France.
[2]CNRS – Université Joseph Fourier Grenoble 1, LGGE UMR 5183, Grenoble, France.
[3]Now at CNRS – Université Laval, Takuvik UMI 3376, Quebec, Quebec, Canada.
[4]Institute of Environmental Physics, University of Heidelberg, Heidelberg, Germany.
[5]Max Planck Institute for Chemistry, Mainz, Germany.
[6]CNRS – Université Joseph Fourier Grenoble 1 – Grenoble INP – IRD, LTHE UMR 5564, Grenoble, France.

0148-0227/12/2011JD016618

emissions from the snowpack on atmospheric chemical reactivity was mostly studied on ice sheets in remote places such as Antarctica and Greenland, where NO_x snowpack emissions are held partly responsible for surprisingly high ozone production rates [*Crawford et al.*, 2001; *Helmig et al.*, 2007; *Legrand et al.*, 2009]. In the marine boundary layer, any ozone photochemical production pathway would be hindered by reactive halogen-catalyzed ozone destruction [*Bauguitte et al.*, 2009]. The potential for chemical interactions between NO_x and reactive halogens was however recognized mostly through modeling studies, which suggested that the hydrolysis of $BrONO_2$, formed through the reaction between NO_2 and BrO, was an important reaction within the catalytic chemical cycle leading to ozone destruction [*Sander et al.*, 1999; *Calvert and Lindberg*, 2003; *Evans et al.*, 2003], and that it contributes to controlling the lifetime of NO_x under conditions where reactive halogens are active [*Saiz-Lopez et al.*, 2007; *Boxe and Saiz-Lopez*, 2008; *Morin et al.*, 2008; *Bauguitte et al.*, 2009]. However, this hypothesis has not been substantiated by strong experimental evidence hitherto.

[3] In this article, we take an isotopic viewpoint to investigate the chemical connection between emissions of NO_x from the snowpack and reactive halogen chemistry. Indeed, dual isotopic analysis of atmospheric nitrate (i.e. the sum of gaseous HNO_3 and particulate nitrate) provides unique insights into NO_x sources and chemical sinks [*Morin et al.*, 2008]. Nitrogen and oxygen isotopic ratios are reported as relative enrichments using the δ scale:

$$\delta = \frac{R_{sample}}{R_{reference}} - 1 \quad (1)$$

where R represents one of the following elemental ratios $n(^{17}O)/n(^{16}O)$, $n(^{18}O)/n(^{16}O)$ or $n(^{15}N)/n(^{14}N)$ in the sample and in a reference, respectively. The reference for oxygen is the Vienna Standard Mean Ocean Water (VSMOW) and for nitrogen it is atmospheric N_2 [*Böhlke et al.*, 2003, and references therein]. For practical reasons δ values are generally expressed in ‰, as variations in isotopic ratios cover a very narrow range.

[4] Nitrogen stable isotope ratios of atmospheric nitrate (expressed in terms of $\delta^{15}N$) are generally used to trace NO_x sources, because the sources imprint different $\delta^{15}N$ signatures [*Kendall et al.*, 2007]. Knowledge about the impact of atmospheric processing of NO_x and nitrate on $\delta^{15}N$ of nitrate is limited and contradictory [*Morin et al.*, 2009], although the conversion of NO_x to nitrate is thought to induce limited ^{15}N isotopic fractionation [*Freyer*, 1991; *Freyer et al.*, 1993]. Field, theoretical and experimental work strongly support that the photolysis of nitrate in snow induces a large negative isotopic fractionation factor [*Blunier et al.*, 2005; *Frey et al.*, 2009]. This means that, during photolysis, ^{15}N-bearing nitrate tends to be preferentially concentrated in the snow phase, while the lighter nitrate isotopologue is preferentially converted into photolytic products such as NO_x and HONO. The subsequent oxidation of these compounds thus leads to atmospheric nitrate exhibiting a $\delta^{15}N$ value much lower than the accepted norm. Indeed, under most atmospheric conditions, $\delta^{15}N$ of atmospheric nitrate ranges between roughly −10 and +10 ‰ [*Morin et al.*, 2009; *Wankel et al.*, 2010; J. Savarino et al., Seasonal variations of isotopic ratios of atmospheric nitrate in the tropical Atlantic Ocean (Cape Verde Observatory, 16°N), manuscript in preparation, 2012]. This is generally interpreted to reflect a narrow range of $\delta^{15}N$ values in atmospheric NO_x under non-polar conditions [*Snape et al.*, 2003; *Morin et al.*, 2009]. In contrast, nitrate formed by oxidation of snowpack-emitted NO_x features a markedly lower $\delta^{15}N$ signature on the order of −40 to −60 ‰ [*Freyer et al.*, 1996; *Wagenbach et al.*, 1998; *Savarino et al.*, 2007; *Morin et al.*, 2008, 2009; *Frey et al.*, 2009; *Savarino and Morin*, 2011]. Thus $\delta^{15}N$ analysis of atmospheric nitrate in the polar lower atmosphere provides a means to track the occurrence of snowpack NO_x emissions into the air mass probed.

[5] The oxygen isotopic composition of nitrate provides information about the nature and the relative importance of NO_x oxidation pathways, ultimately leading to atmospheric nitrate. In the atmosphere, the ozone molecule possesses a unique isotopic singularity, referred to as the isotope anomaly, originating from non-mass dependent fractionation during its formation in the atmosphere [*Thiemens*, 2006; *Marcus*, 2008, and references therein]. In this study the isotope anomaly $\Delta^{17}O$, also referred to as the ^{17}O-excess, is defined as:

$$\Delta^{17}O = \delta^{17}O - 0.52 \times \delta^{18}O \quad (2)$$

$\Delta^{17}O$ is a conserved variable in the atmosphere, i.e. it is not significantly influenced by mass-dependent fractionation [*Kaiser et al.*, 2004; *Thiemens*, 2006; *Kendall et al.*, 2007; *Morin et al.*, 2011]. Therefore $\Delta^{17}O$ of atmospheric species unambiguously traces the influence of ozone in their chemical formation pathways [e.g., *Brenninkmeijer et al.*, 2003; *Thiemens*, 2006, and references therein]. Homogeneous NO_x oxidation by the OH radical leads to the lower range of $\Delta^{17}O$ values, while heterogeneous nitrate production (N_2O_5 or $BrONO_2$ hydrolysis) or homogeneous channels involving the nitrate radical NO_3 lead to higher $\Delta^{17}O$ values (see details in work by *Michalski et al.* [2003], *Morin et al.* [2007b, 2009], *Kunasek et al.* [2008]). Until a consistent and rigorous framework for the quantitative modeling of $\Delta^{17}O$ values, fully adapted to polar conditions, has emerged [*Kunasek et al.*, 2008; *Morin et al.*, 2011], $\Delta^{17}O$ data are used as a qualitative indication of the NO_x oxidative conditions in a given air parcel, consistent with similar past studies [*Michalski et al.*, 2003; *Morin et al.*, 2007a, 2007b, 2008, 2009; *Savarino et al.*, 2007; *Kunasek et al.*, 2008; *Alexander et al.*, 2009].

[6] In this article, we neither present nor discuss $\delta^{18}O$ values because their interpretation in terms of NO_x oxidation pathways is partly redundant with and significantly more ambiguous than $\Delta^{17}O$ [*Morin et al.*, 2008, 2009; *Jarvis et al.*, 2008]. One peculiarity of the polar atmosphere is that, during summer and winter, photochemical conditions exhibit little diurnal variations, in contrast to the situation encountered in midlatitudes. This situation reinforces the seasonal contrast in terms of $\Delta^{17}O$ between the daytime and nighttime nitrate production channels [*Michalski et al.*, 2003; *Morin et al.*, 2008]. However, this consideration is modulated by the fact that a significant fraction of atmospheric nitrate found in the polar atmosphere stems from long-range transport, which carries an isotopic signature representative of its source region [*Morin et al.*, 2008].

[7] Past efforts to interpret the dual isotopic composition of atmospheric nitrate ($\delta^{15}N$, $\Delta^{17}O$) in the Arctic boundary layer reached the following conclusions:

[8] 1. The $\delta^{15}N$ displays an asymmetrical seasonal cycle, with a maximum in summer on the order of 0–5 ‰, and a minimum in winter on the order of −10 to −15 ‰, both in the MBL at Alert, Nunavut, Canada, and at Summit on the Greenland plateau [*Hastings et al.*, 2004; *Morin et al.*, 2008]. Atmospheric measurements at Alert display a significant drop in $\delta^{15}N$ during the springtime, down to −42 ‰ [*Morin et al.*, 2008]. The time period showing low $\delta^{15}N$ values matches the time period when both UV light and seasonal snow are simultaneously present, at the scale of the Arctic basin [*Morin et al.*, 2008].

[9] 2. $\Delta^{17}O$ displays an asymmetrical seasonal cycle, with a minimum in summer, on the order of 24–26 ‰, and a maximum in winter, on the order of 30–32 ‰, both in the MBL and on the Greenland plateau [*Kunasek et al.*, 2008; *Morin et al.*, 2008]. Even higher values were found during springtime in the MBL, on the order of 33–35 ‰. It was concluded that only the hydrolysis of $BrONO_2$ could explain such high values of $\Delta^{17}O$ at this time of the year [*Morin et al.*, 2007b, 2008].

[10] 3. Based on simultaneous measurements of $\Delta^{17}O$ and $\delta^{15}N$ at the semi-weekly timescale in the MBL, it was realized that low $\delta^{15}N$ values were a prerequisite for observing high $\Delta^{17}O$ values. In other words, the semi-weekly isotopic record from Alert was indicative of the fact that oxidation of NO_x by reactive halogens was only possible in the presence of a locally produced NO_x, which can only be supplied by the photodenitrification of the snowpack [*Morin et al.*, 2008, 2009].

[11] 4. One study has reported that microbial denitrification in the snowpack could contribute significantly to the budget of reactive nitrogen in the Arctic [*Amoroso et al.*, 2010], based on dual isotopic measurements of nitrate in the snow (in particular $\Delta^{17}O$ values close to zero, which can only be produced biologically within the snowpack) and concomitant reactive nitrogen fluxes from the snowpack in the dark (i.e., of non photochemical nature). The broader relevance of this finding to the reactive nitrogen biogeochemical cycle in Arctic regions awaits further evaluation.

[12] Atmospheric nitrate was sampled at a daily time resolution during the Barrow 2009 campaign carried out under the auspices of the OASIS (Ocean–atmosphere-Sea ice-Snowpack) project in spring 2009 at Barrow, Alaska, USA. The aim was to refine and possibly strengthen the isotopic evidence for chemical coupling between NO_x emissions and reactive halogen chemistry, so far based on a sole semi-weekly data set from Alert, Nunavut, Canada [*Morin et al.*, 2008] and indirect evidence from a few daily samples from Ny Ålesund, Svalbard [*Morin et al.*, 2009]. Furthermore, sampling continued on at a weekly time resolution until February 2010, leading to a complementary data set to constrain seasonal variations of $\delta^{15}N$ and $\Delta^{17}O$ in the High Arctic. The results are presented in this article, and contrasted with the other data available from the Arctic lower atmosphere.

2. Experimental Setup

2.1. Sample Collection

[13] The atmospheric nitrate samples were collected at Barrow, Alaska, USA (71°N, 156°W) by means of high-volume (HiVol) air sampling. The air was pumped at a flow rate of 1.1 m^3 min^{-1} through a single cellulose acetate Whatman 41 filter (12.7 × 17.8 cm). Such types of filters are assumed to retain both gas-phase HNO_3 and particulate nitrate, the sum of which is referred to as atmospheric nitrate hereinafter [*Morin et al.*, 2007b]. In addition, these filters are similar to what has been consistently used at Alert for aerosol monitoring [*Sirois and Barrie*, 1999], including the previous study by *Morin et al.* [2008]. The HiVol sampler was installed on the roof of the Barrow Arctic Research Consortium (BARC) building near Barrow, about 500 m away from the sea shore. There, filters were changed daily from 3 March 2009 to 12 April 2009, during the OASIS 2009 intensive field campaign. The sampler was relocated at the NOAA Observatory, a few km to the north–east of the main settlement, on 14 April 2009, on a platform behind the building, approximately 2 meters above the snow surface. There, filters were changed approximately every week until 10 February 2010. The filter set thus consists in 32 filters collected at a daily resolution in March–April 2009 and 40 weekly samples covering the period April 2009–February 2010. The filters were stored frozen individually in sealed plastic bags and shipped to Grenoble, France, for analysis, at the end of the sampling campaign.

2.2. Chemical and Isotopic Analyses

[14] Soluble species deposited on the filters were dissolved in ultrapure water (18 MΩ cm^{-1}) under ultra-clean conditions [*Morin et al.*, 2007b]. All subsequent analyses were performed on nitrate dissolved during this step. Nitrate concentrations were determined in filter extracts using a colorimetric method, with a reported uncertainty of approximately 5% in the range 10–100 ng g^{-1} [*Patey et al.*, 2008]. Atmospheric concentrations were derived by dividing the mass of nitrate recovered on the filters by the total sampled air volume not corrected for temperature and pressure variations around the standard temperature and pressure conditions. The contribution of sampling blanks was always found to be negligible.

[15] Nitrogen and oxygen isotopic ratios were measured using the automated denitrifier method, as described by *Morin et al.* [2009]. This method was initially developed by *Sigman et al.* [2001] and *Casciotti et al.* [2002], and adapted by *Kaiser et al.* [2007] to the measurement of the comprehensive ($^{17}O/^{16}O$ and $^{18}O/^{16}O$) oxygen isotopic composition of nitrate. The technique uses *Pseudomonas aureofaciens* bacteria to convert nitrate into N_2O, which is analyzed for its isotopic composition after being thermally decomposed into O_2 and N_2 in a gold tube. The analytical procedure used for this study is strictly identical to the description given by *Morin et al.* [2009]. Uncertainties pertaining to the $\delta^{18}O$, $\Delta^{17}O$ and $\delta^{15}N$ values are 1.8 ‰, 0.5 ‰, and 0.4 ‰, respectively.

2.3. Data Reduction and Complementary Data

[16] The data presented in this study and used for assessing seasonal variations were resampled into 10-day and monthly weighted averages. The same treatment was applied to previous data sets obtained in the Arctic MBL [*Morin et al.*, 2007a, 2007b, 2008]. This approach allows for the comparison of data sets originally obtained at various time resolutions.

[17] The mixing ratio of BrO was measured at the surface using long-path differential optical absorption spectroscopy

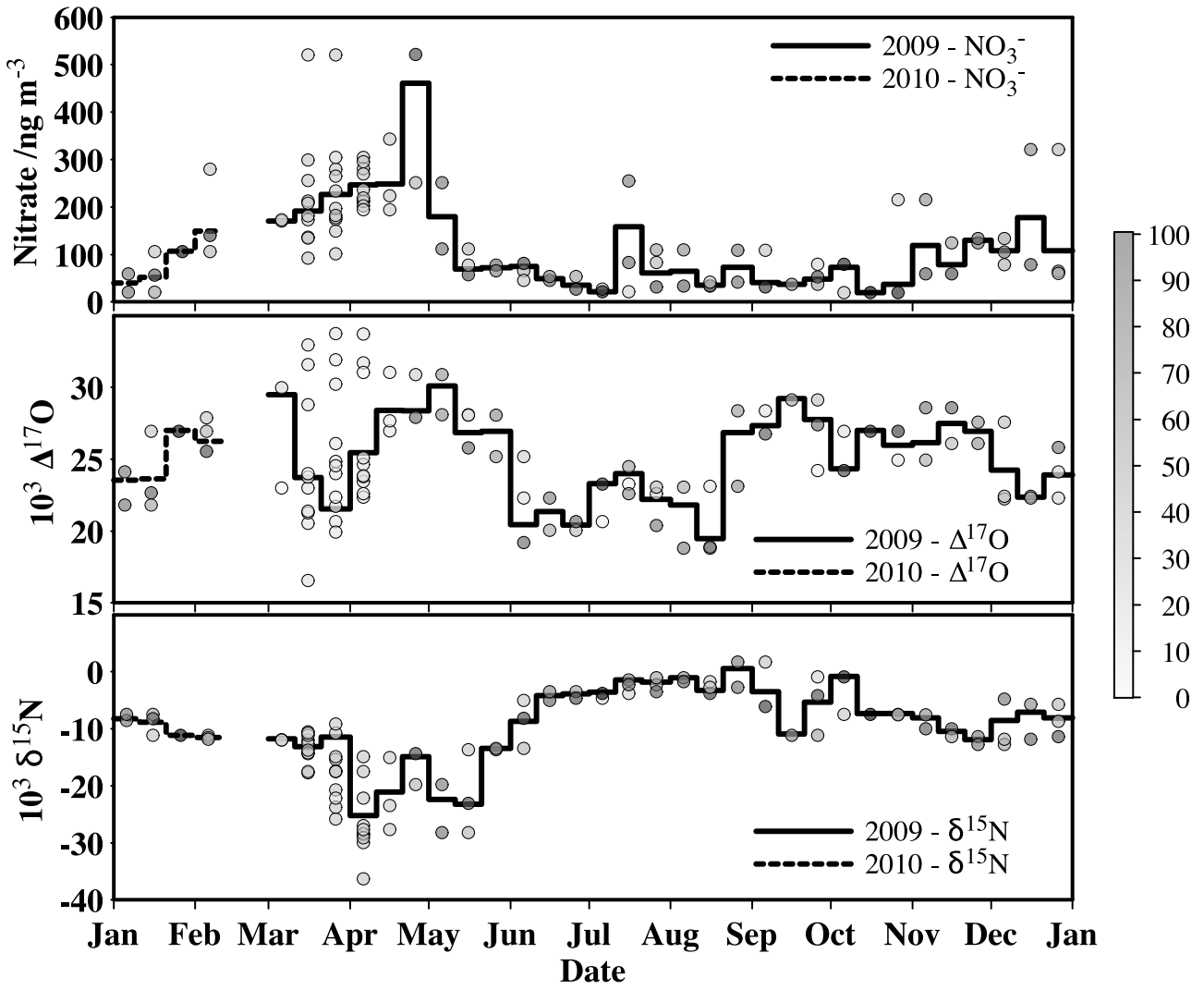

Figure 1. Time series of the (top) nitrate concentration, (middle) $\Delta^{17}O$ and (bottom) $\delta^{15}N$ at Barrow, Alaska, between March 2009 and February 2010. The solid and dashed lines represent the data resampled as a nitrate mass weighted average over 10-day time periods in 2009 and 2010, respectively. Dots represent individual filter samples, color-coded with the percentage of time they contribute to each 10-day averaging periods. Note that a single filter sample can contribute to up to three 10-day time periods. The end of the sampling period, namely January and February 2011, is presented on the left of the graph, so that the seasonal cycle is resolved using a similar abscissa than in subsequent plots.

LP-DOAS [*Liao et al.*, 2011]. For this study, the time-resolution of the LP-DOAS data has been reduced to hourly averages. Full details about the LP-DOAS measurements at Barrow during the OASIS campaign are provided by *Liao et al.* [2011] and *Friess et al.* [2011].

[18] Complementary data used for this work consist of meteorological, surface ozone and radiation data measured at and provided by the NOAA Observatory at Barrow.

3. Results

3.1. Seasonal Variations of $\delta^{15}N$ and $\Delta^{17}O$ of Nitrate at Barrow, Alaska

[19] Figure 1 shows the seasonal variations of the concentration of atmospheric nitrate in the Barrow air, along with its $\delta^{15}N$ and $\Delta^{17}O$ values, as recorded between March 2009 and February 2010. To provide context for these data, Figures 2 and 3 display seasonal variations of $\delta^{15}N$ and $\Delta^{17}O$, respectively, at several Northern Hemisphere locations. $\delta^{15}N$ values are contrasted with seasonal variation from Alert, Nunavut (82.5°N, 62.4°W) [*Morin et al.*, 2008], which is the other Arctic MBL site where year-round $\delta^{15}N$ data are available. Data from the Gulf of Aqaba (29.5°N, 34.9°E) [*Wankel et al.*, 2010], where atmospheric nitrate $\delta^{15}N$ data have recently been obtained, are also included for comparison. $\Delta^{17}O$ data are compared to year-round data from Alert, Nunavut [*Morin et al.*, 2007b, 2008], previous data obtained at Barrow, Alaska in spring 2005 [*Morin et al.*, 2007a] and data from La Jolla, California (32.8°N, 117.3°W) [*Michalski et al.*, 2003]. Monthly averaged concentrations, $\Delta^{17}O$ and $\delta^{15}N$ data from Barrow 2009–2010 (this study), Alert 2004 [*Morin et al.*, 2007b] and Alert 2005–2006 [*Morin et al.*,

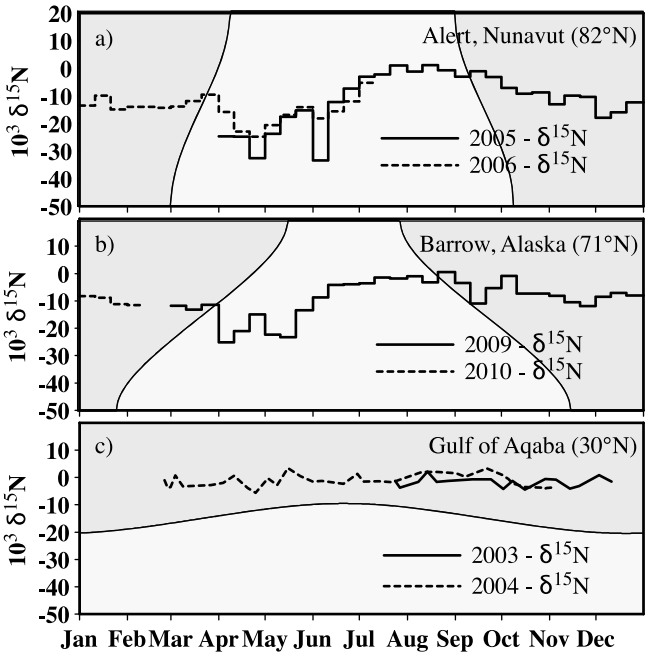

Figure 2. Time series of the seasonal variation of δ^{15}N of atmospheric nitrate at (a) Alert, Nunavut, 82°N [*Morin et al.*, 2008], (b) Barrow, Alaska, 71°N (this study) and (c) the coast of the Gulf of Aqaba, 29.5°N, 34.9°E [*Wankel et al.*, 2010]. Note that data from Alert and Barrow are resampled over 10-day time periods to facilitate comparison between data sets of various sampling resolution. The relative duration of day and night is represented by shaded areas.

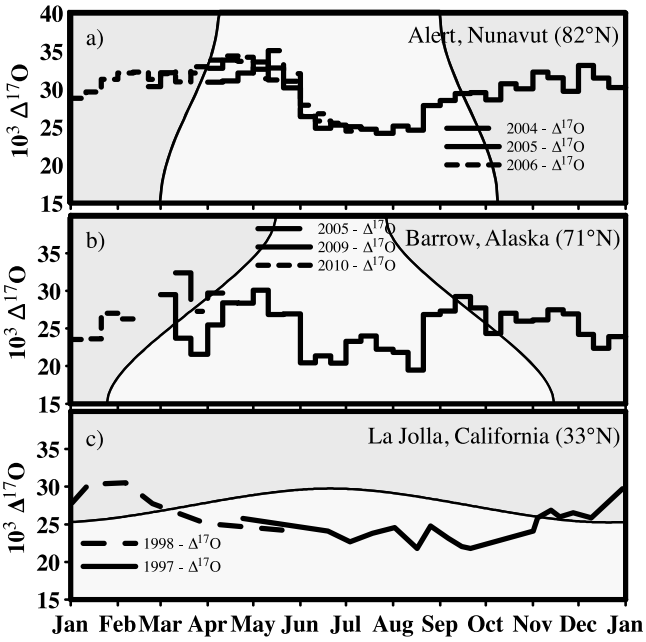

Figure 3. Time series of the seasonal variation of Δ^{17}O of atmospheric nitrate at (a) Alert, Nunavut, 82°N [*Morin et al.*, 2007b, 2008], (b) Barrow, Alaska, 71°N [*Morin et al.*, 2007a] (also this study) and (c) La Jolla, California, 32.8°N, 117.3°W [*Michalski et al.*, 2003]. Note that data from Alert and Barrow are resampled over 10-day time periods to facilitate comparison between data sets of various sampling resolution. The relative duration of day and night is represented by shaded areas.

2008] are provided in Tables 1 and 2 to facilitate future use such as model evaluation [*Alexander et al.*, 2009] or data compilation.

3.1.1. Concentrations of Atmospheric Nitrate

[20] Nitrate concentrations exhibit a seasonal maximum between March and May, consistent with previous studies dealing with Arctic Haze at Barrow, Alaska [see, e.g., *Quinn et al.*, 2007]. During this time period, while the concentration of nitrate in individual (daily) samples can amount up to 500 ng m^{-3}, 10-day averages are on the order of 200 to 300 ng m^{-3}. The rest of the year, nitrate concentrations are typically on the order of or lower than 100 ng m^{-3}. Concentrations are minimal in summer, between July and October, when nitrate concentrations remain on the order of 50 ng m^{-3}. We believe that our measurements carried out on atmospheric nitrate are insignificantly impacted by the presence of the town of Barrow. Indeed, nitrate is not emitted primarily from anthropogenic activities, but results secondarily from the atmospheric oxidation of gaseous precursors such as NO_x [*Finlayson-Pitts and Pitts*, 2000]. The proximity of the sampling area to the town precludes significant impact of in-plume oxidation of local anthropogenic NO_x into atmospheric nitrate. This reasoning would of course not hold for primary aerosol species.

3.1.2. The δ^{15}N of Atmospheric Nitrate

[21] The δ^{15}N of nitrate for the Barrow 2009–2010 sampling campaign exhibits a seasonal maximum in summer, reaching values between −2 and 0 ‰ during July, August and September. Winter values are on the order of −10 ‰. During springtime, δ^{15}N value are significantly lower, with 10-day averages remaining in the range (−25‰; -15‰) from March to May. Individual δ^{15}N values reach a minimal value

Table 1. Monthly Averaged Data From the Nitrate Isotopic Measurements Carried Out at Alert From 2004 to 2006[a]

Year	Month	Prop.	Conc.	δ^{18}O	Δ^{17}O	δ^{15}N
2004	February	8.2	65.7	71.8	30.3	
	March	90.1	76.5	80.1	32.2	
	April	99.9	118.9	86.4	33.4	
	May	76.0	92.6	85.7	32.7	
	June	26.1	112.5	71.3	27.8	
2005	April	87.7	208.0	81.2	31.6	−28.6
	May	99.7	149.7	86.5	32.6	−19.6
	June	100.0	42.7	71.0	25.6	−19.1
	July	99.9	38.6	70.4	24.8	−2.1
	August	100.0	39.8	72.2	25.8	−0.6
	September	100.0	26.6	73.2	29.3	−2.3
	October	100.0	21.0	71.1	30.0	−8.5
	November	100.0	78.3	71.0	30.9	−11.1
	December	100.0	123.9	75.0	31.5	−15.4
2006	January	100.0	106.3	65.3	30.0	−12.6
	February	99.9	131.3	73.3	32.0	−14.0
	March	99.9	173.2	78.4	31.9	−11.6
	April	99.8	170.9	88.3	34.1	−20.9
	May	99.5	130.2	84.6	31.8	−17.9
	June	100.0	48.5	69.9	26.0	−15.8
	July	31.0	20.0	66.7	24.5	−5.2

[a]See section 2.1 for details. Prop. refers to the proportion of time in a given month covered with measurements, in %. Conc. refers to the concentration of nitrate, in ng m^{-3}. Isotopic data are reported in ‰.

Table 2. Monthly Averaged Data From the Nitrate Isotopic Measurements Carried Out at Barrow From 2009 to 2010[a]

Year	Month	Prop.	Conc.	$\delta^{18}O$	$\Delta^{17}O$	$\delta^{15}N$
2009	March	65.6	206.5	55.3	22.9	−12.2
	April	68.2	342.0	67.2	27.5	−18.7
	May	100.0	106.0	70.3	28.6	−20.4
	June	100.0	52.9	48.1	20.7	−6.2
	July	100.0	79.8	60.1	23.5	−1.7
	August	100.0	58.1	60.6	23.6	−0.7
	September	76.9	43.7	70.3	27.8	−5.5
	October	100.0	43.0	59.4	25.2	−3.8
	November	100.0	108.9	58.4	26.8	−10.2
	December	100.0	130.4	46.1	23.3	−7.8
2010	January	100.0	67.7	53.6	25.5	−10.0
	February	35.4	149.6	58.7	26.3	−11.5

[a]See section 2.1 for details. Prop. refers to the proportion of time in a given month covered with measurements, in %. Conc. refers to the concentration of nitrate, in ng m^{-3}. Isotopic data are reported in ‰. Data from Barrow 2005 [*Morin et al.*, 2007a] are not presented since they cover less than 25 % of the month of March 2005.

of −36 ‰ during the first 10-day period of April. In addition to these general features, September stands out with a rather large variability ($\delta^{15}N$ ranging between −3 and −11 ‰). This general behavior is consistent with data previously collected at Alert, Nunavut, displaying similar seasonality. The main differences between the Alert and Barrow seasonal variations of $\delta^{15}N$ is the earlier drop of $\delta^{15}N$ at the beginning of spring at Barrow than at Alert. Finally, the Alert data set does not display the small $\delta^{15}N$ dip which is visible in September in the Barrow data-set. In contrast to both Arctic sites showing similar seasonality, it is worth realizing that mid-latitude and tropical sites exhibit a much lower variability in terms of $\delta^{15}N$: the Gulf of Aqaba data show $\delta^{15}N$ ranging between −6 and 4 ‰. Unpublished data on the seasonal variations of $\delta^{15}N$ at the Cape Verde Observatory (16.8°N, 24.8°W) (Savarino et al., manuscript in preparation, 2012) give seasonal $\delta^{15}N$ variations between −8 and −3 ‰. Both of these non-Arctic sites display a weak seasonal cycle. In light of the small range of variation exhibited by atmospheric nitrate under non-Arctic conditions and the precision of the analytical method, the variability observed in September at Barrow is thus considered significant. We note that one such anomalous 10-day period can also be spotted in the Alert data-set in December 2005, although the deviation to the seasonal cycle of $\delta^{15}N$ is smaller.

[22] Both Arctic $\delta^{15}N$ cycles feature a maximum in summer and a minimum in winter, not considering the disturbance in a periodic seasonal profile induced by the low values found during spring. This deviation happens in April and May at Barrow, and from April to June at Alert. Excluding these periods of time from the following analysis, to further compare the seasonal variations of $\delta^{15}N$ at Alert and Barrow, the data were fitted to the following cosine function:

$$\delta^{15}N(t) = \delta^{15}N_0 + \delta^{15}N_a \times (1 + \cos(\omega t + \phi))/2 \quad (3)$$

In this equation, t is the fractional date of the year, starting on 21 December, i.e. the winter solstice, $\delta^{15}N_0$ represents the maximum value of the seasonal cycle, $\delta^{15}N_a$ is the peak-to-peak amplitude of the seasonal variations of $\delta^{15}N$, ω represents the angular frequency corresponding to a yearly period of variation, ϕ represents a potential phase difference between the seasonal cycle of solar radiation at the surface and $\delta^{15}N$. This approach allows a better quantification of the range and phase of the seasonal variations of $\delta^{15}N$. The 10-day average values of $\delta^{15}N$ of atmospheric nitrate collected at Barrow were fitted to the data using a least squares method. The results of the fit are summarized in Table 3. Within the uncertainty pertaining to the fit parameters, the seasonal maximum of $\delta^{15}N$ is rather similar at Alert and Barrow, on the order of −2 ‰. The seasonal amplitude of $\delta^{15}N$ is wider at Alert (ca. 14 ‰) than at Barrow (ca. 8 ‰). Last, the timing of the seasonal maximum is similar within the uncertainty of the regression analysis, and it occurs in late July for both time series.

3.1.3. $\Delta^{17}O$ of Atmospheric Nitrate

[23] The Barrow 2009–2010 data of $\Delta^{17}O$ of nitrate exhibit a seasonal minimum during summer, featuring $\Delta^{17}O$ values on the order of 20–22 ‰. In winter, $\Delta^{17}O$ rises up to values ranging between 25 and 27 ‰. The springtime period exhibits a wide range of $\Delta^{17}O$ values: data from individual samples span the interval 16–34 ‰ (see Figure 1). The 10-day averages are then also highly variable and range between 22 and 30 ‰. A comparison to the Alert data set reveals that the Barrow data follow overall the same pattern, although the Barrow data-set also displays more variability than the Alert data throughout the year. The seasonal cycle of $\Delta^{17}O$ at Alert was smoother and almost perfectly reproducible from year to year, as evidenced by the data gathered on three consecutive springtimes (see Figure 3). In addition, the $\Delta^{17}O$ values tend to be lower at Barrow than at Alert, with an offset on the order of 2 to 3 ‰ throughout the year. The Barrow data also show more inter-annual variability: data for spring 2009 appear lower on average than for the spring 2005, although they both cover the same range except for the highest 10-day period of spring 2005. No known experimental artifact can explain such lower values. Repeated measurements on sets of samples analyzed previously have not revealed any trend or bias in the analytical procedure, leading to the conclusion that the Barrow 2009–2010 measurements are robust and can be compared to other measurements.

[24] At La Jolla, $\Delta^{17}O$ clearly features a seasonal maximum in winter (ca. 32 ‰) and a seasonal minimum in summer (ca. 20 ‰) [*Michalski et al.*, 2003]. At the Cape Verde Observatory (Savarino et al., manuscript in preparation, 2012), $\Delta^{17}O$ data range between 25 and 30 ‰ without a clear seasonal pattern. Seasonal variations are smooth in both cases.

3.2. Daily Variations of $\delta^{15}N$ and $\Delta^{17}O$ at Barrow, Alaska, During the Intensive OASIS 2009 Field Campaign

[25] Figure 4 shows the high-resolution record of $\delta^{15}N$ and $\Delta^{17}O$ of atmospheric nitrate during the OASIS 2009 field

Table 3. Fit Parameters of the Regression of the Seasonal Cycle of $\delta^{15}N$ to Function $\delta^{15}N(t) = \delta^{15}N_0 + \delta^{15}N_a \times (1 + \cos(\omega t + \phi))/2$[a]

Location	Alert 2005–2006	Barrow 2009–2010
$\delta^{15}N_0$	−1.0 ± 0.8 ‰	−3.1 ± 0.8 ‰
$\delta^{15}N_a$	−13.7 ± 1.1 ‰	−8.4 ± 1.3 ‰
ϕ/rad	−0.52 ± 0.11	−0.73 ± 0.18
ϕ/week from 21 June	late by 4 ± 1 weeks	late by 6 ± 1 weeks
number of 10-day periods used	29	28

[a]The data are from the Alert 2005–2006 and Barrow 2009–2010 seasons. Low $\delta^{15}N$ values from April and May were excluded from the fit calculation. At Alert, June was also excluded.

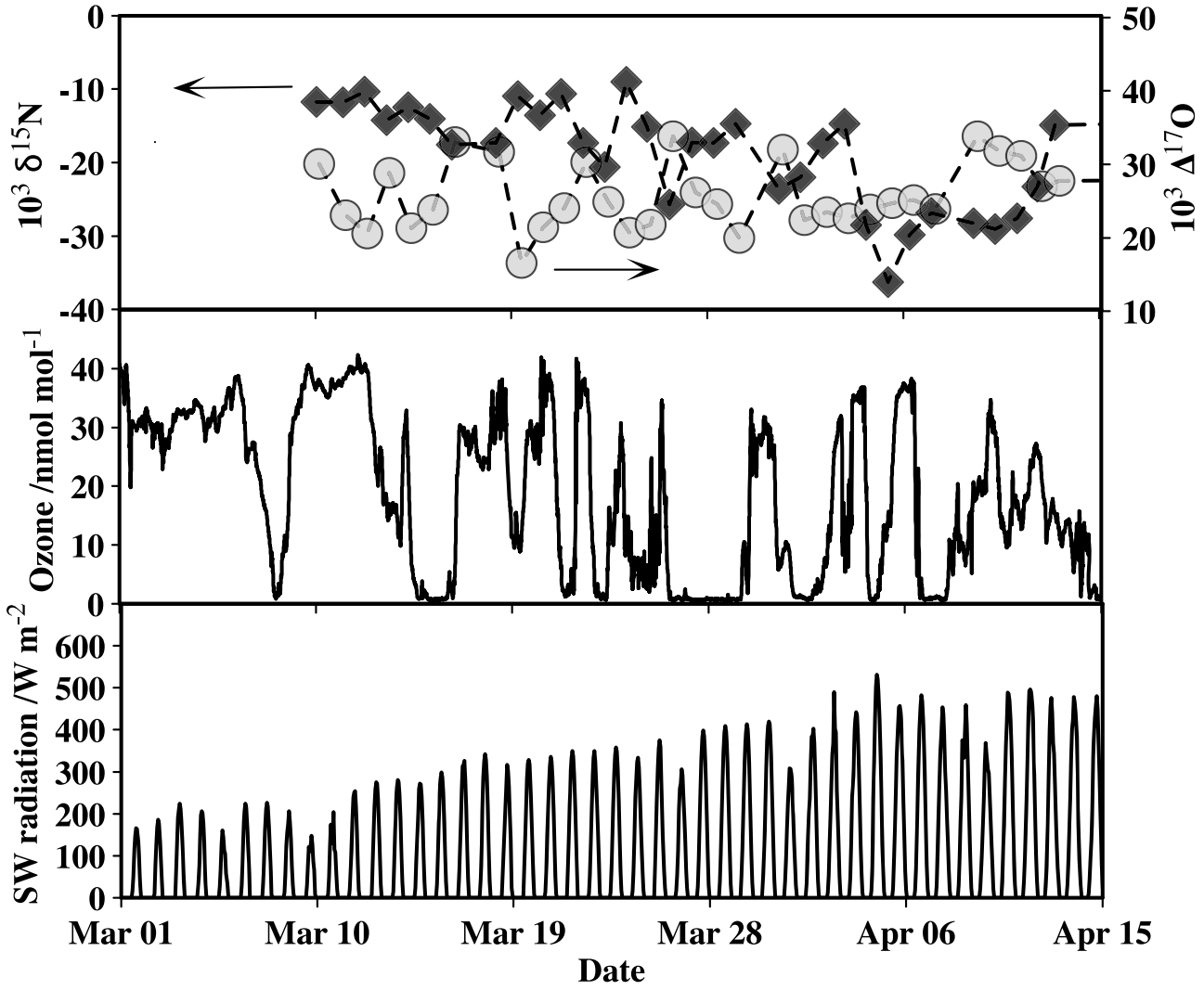

Figure 4. Time series of the variation of $\Delta^{17}O$ (circles) and $\delta^{15}N$ (diamonds) during the intensive OASIS 2009 field campaign at Barrow, Alaska. Also shown are the mixing ratio of ozone and the short-wave radiation at the surface (data courtesy of NOAA ESRL).

campaign (March and April 2009), along with the mixing ratio of ozone and incoming short-wave radiation at the surface (both courtesy of NOAA ESRL). This plot clearly shows the occurrence of several strong and sustained ozone depletion events (e.g. on 15 March and from 26 to 30 March). During this entire time period, $\delta^{15}N$ and $\Delta^{17}O$ both exhibit a strong variability. $\delta^{15}N$ remained relatively steady at the beginning of the sampling campaign, around -12 ‰ until 15 March. It then started to show several marked decreases, down to -36 ‰, in early April. Similarly, $\Delta^{17}O$ displayed marked day-to-day variations during this time period, showing values ranging between 16 and 34 ‰, which exceeds the known range of the seasonal variation of $\Delta^{17}O$ at midlatitude sites [*Michalski et al.*, 2003; Savarino et al., manuscript in preparation, 2012] ca. from 20 to 32 ‰; see Figure 3c.

[26] The Arctic spring time period is the period of the year where the variability of the mixing ratio of ozone maximizes, due to the occurrence of frequent ozone depletion events [*Bottenheim et al.*, 2009; *Friess et al.*, 2011]. This study confirms that $\delta^{15}N$ and $\Delta^{17}O$ display the strongest variability when the ozone concentration is most variable. A linear correlation between $\Delta^{17}O$ of nitrate and the mixing ratio of ozone was found at Alert during springtime 2004 [*Morin et al.*, 2007b]. Figure 5 shows $\Delta^{17}O$ versus the averaged mixing ratio of ozone during the aerosol sampling periods, at Alert, between 15 March and 31 May in 2004, 2005 and 2006. It indicates that the correlation found in 2004 on a subset of the whole springtime period has not been observed in the following years and may therefore be considered coincidental. Likewise, we do not observe a direct correlation between the mixing ratio of ozone and $\Delta^{17}O$ from the daily Barrow 2005 and 2009 data-sets, as partially presented by *Morin et al.* [2007a] and shown in Figure 6. Figure 7 shows the time series of $\Delta^{17}O$ along with the hourly variations in BrO at the surface. Most peaks in the time series of the mixing ratio of BrO correspond to a corresponding maximum of $\Delta^{17}O$ of nitrate at the daily time resolution. There thus seems to exist, at least qualitatively, a relationship between the BrO mixing ratio and $\Delta^{17}O$. However, when BrO data are averaged over each aerosol

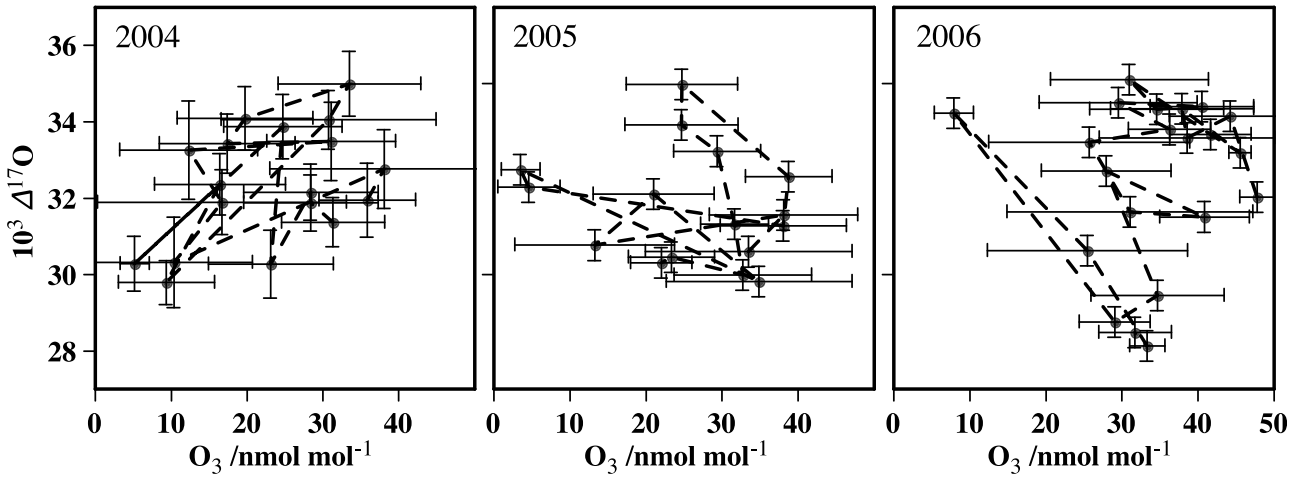

Figure 5. $\Delta^{17}O$ versus the mixing ratio of ozone during the aerosol sampling interval, for the period between 15 March and 31 May for three consecutive years at Alert, Nunavut. Note that the correlation between the two variables, exhibited by *Morin et al.* [2007b], was not seen during the two following springtime periods. Horizontal error bars represent the variability of the mixing ratio of ozone within each aerosol sampling period. Vertical error bars represent the analytical uncertainty pertaining to $\Delta^{17}O$ measurements. Dashed lines link consecutive measurements.

sampling period, no significant correlation is found between averaged BrO data and $\Delta^{17}O$, similar to what is described for ozone above.

4. Discussion

4.1. Seasonality of Snowpack Emissions of NO_x in the Arctic MBL

[27] There is currently ample evidence to support the fact that strongly negative (i.e., lower than −20 ‰) $\delta^{15}N$ in atmospheric nitrate traces the process whereby NO_x is photochemically emitted from the snowpack and subsequently oxidized into atmospheric nitrate [*Frey et al.*, 2009, and references therein]. Such low values fall significantly outside the range of $\delta^{15}N$ values commonly found at non-polar sites. *Morin et al.* [2008] evaluated the seasonality of the snowpack emissions of NO_x in the Arctic MBL using a full year of $\delta^{15}N$ measurements from Alert, Nunavut. The principle of the analytical framework developed by *Morin et al.* [2008] relied on computing the deviation of the $\delta^{15}N$ measured values from the seasonal cycle. The latter was computed using a regression of $\delta^{15}N$ against air temperature at Alert. As shown above, here the seasonal cycle is built on a cosine function so that fit parameters can be compared between Arctic locations. $\delta^{15}N$ deviations from the idealized seasonal cycles are shown in Figure 8. Positive values on this graph are indicative of a significant contribution of the snowpack NO_x source.

[28] According to Figure 8, the time period of the year during which the budget of atmospheric nitrate is influenced by photochemical NO_x emissions is longer at Alert, Nunavut (90 days, i.e. nine 10-day periods) than at Barrow, Alaska (50 days, i.e. five 10-day periods). It is worth noting that the Barrow data-set exhibits one 10-day period in September when $\delta^{15}N$ also significantly deviated from the seasonal cycle; such a secondary deviation from the seasonal cycle of $\delta^{15}N$ was not evident in the Alert data-set. This could also be indicative of NO_x emissions from the snowpack during this season of the year.

[29] The necessary ingredients for photochemical emissions of NO_x from the snowpack are a nitrate-containing snow cover and UV radiation. Based on this simple consideration, *Morin et al.* [2008] showed that the period of the year when snowpack emissions of NO_x makes a significant contribution to the budget of atmospheric nitrate corresponds to the maximum of the snow illumination index calculated as follows:

$$\mathrm{SII}(t) = \alpha \times \mathrm{SCA}(t) \times F_{\mathrm{UV}}(t) \quad (4)$$

where SCA is the snow cover area at the scale of the Arctic basin, F_{UV} is the daily integrated UV radiation reaching the surface at a given latitude, and α is a normalization coefficient so that SII is both non-dimensional and ranges between 0 and 1. In winter, SII is zero because there is no light in the Arctic. In summer, SII is also zero because snow is absent over most continental landmasses and sea ice. SII thus maximizes only in springtime. Based on satellite-derived SCA estimates at the scale of the Arctic basin (including snow covered sea-ice) [*Drobot and Anderson*, 2001; *Robinson and Frei*, 2000] and on idealized erythemal UV fluxes reaching the surface at 80°N, SII was found to peak when $\delta^{15}N$ deviates from the seasonal cycle [*Morin et al.*, 2008]. Here this analysis is repeated, using the same data except that the Barrow data are compared to SII estimates using the seasonal cycle of UV radiation computed at 70°N. The result of the computation taking into account the UV radiation at 70°N and 80°N is shown on Figure 9. Figure 9 shows that our rough analysis is consistent with the $\delta^{15}N$ observations: the NO_x snowpack emissions season starts earlier at 70°N than at 80°N, owing to earlier polar sunrise. However, since the timing for snowmelt is represented similarly in the two computations, this analysis does not reproduce the fact that snowpack emissions of NO_x last longer at

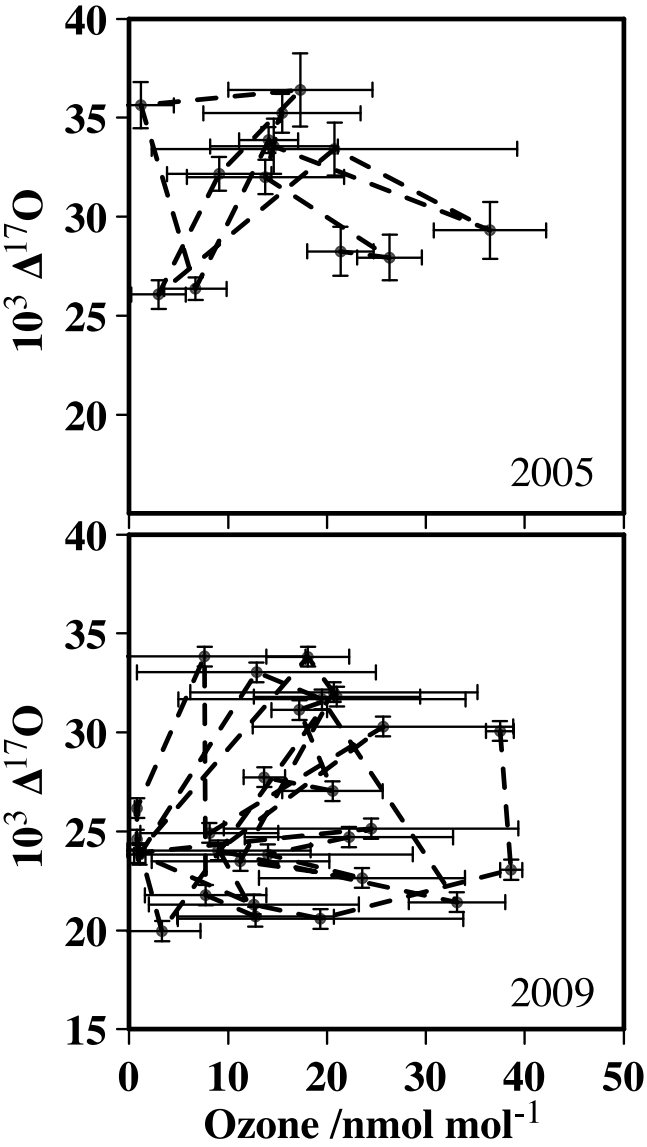

Figure 6. $\Delta^{17}O$ versus the mixing ratio of ozone during the aerosol sampling interval, in (top) March 2005 and (bottom) March and April 2009 at Barrow, Alaska. Measurements from 2005 are taken from the data-set used by *Morin et al.* [2007a]. Horizontal error bars represent the variability of the mixing ratio of ozone within each aerosol sampling period. Vertical error bars represent the analytical uncertainty pertaining to $\Delta^{17}O$ measurements. Dashed lines link consecutive measurements.

80°N than at 70°N. Last, the rough analysis reveals that the September $\delta^{15}N$ deviation observed at Barrow is consistent with the onset of snow season being simultaneous with sufficient UV levels to promote the photolysis of nitrate.

[30] The rough analysis based on general statistics of seasonal snowpack onset and melt, and idealized UV radiation at the surface in two latitudinal bands, reproduces fairly well the observed pattern of $\delta^{15}N$ deviations from the seasonal cycle. This provides a first evaluation that $\delta^{15}N$ of nitrate is a good indicator for significant NO_x emissions from the snowpack at the regional scale. Nevertheless, an in-depth analysis of surface and atmospheric conditions conducive to NO_x emissions from the snowpack could be achieved by combining simultaneous estimates of snow cover, surface UV-radiation along with air mass back trajectories. Such an analysis would for instance allow to verify whether snow covered sea ice surfaces play a different role than continental snow in terms of photochemical NO_x emissions, which has recently been suggested on the basis of atmospheric observations of NO_x in the Hudson Bay [*Moller et al.*, 2010]. The analysis presented here does not allow for the precise discrimination between the types of surfaces involved, although previous isotopic work including back-trajectory analysis did not indicate any influence of the type of snow covered area in terms of potential for photochemical NO_x release [*Morin et al.*, 2009].

[31] *Amoroso et al.* [2010] reported that microbial denitrification could occur in the snowpack, based on a combination of reactive nitrogen flux measurements and isotopic measurements of nitrate in the snowpack at Ny Ålesund, Svalbard. We find no evidence that this process has taken place during the sampling periods of the present study; however, this statement is inconclusive due to the lack of isotopic analysis of snowpack nitrate, which was a crucial contribution to the conclusions of *Amoroso et al.* [2010].

4.2. Seasonality of Reactive Halogen Chemistry in the Arctic MBL

[32] The seasonal cycle of $\Delta^{17}O$ at Barrow features a higher variability than at Alert. Indeed, as evidenced in Figure 3, the variability of $\Delta^{17}O$ data from Barrow, based on 10-day averages, is larger at Barrow that at Alert. $\Delta^{17}O$ is used as a tracer for NO_x oxidation pathways, and is thus highly sensitive to photochemical conditions in the air masses where nitrate is produced [*Michalski et al.*, 2003; *Alexander et al.*, 2009; *Morin et al.*, 2011]. The large variability in $\Delta^{17}O$ values observed at Barrow thus indicates a large variability in the photochemical conditions prevailing in the air masses sampled. Compared to Alert, the main reason for this difference in variability is due to the fact that Barrow is situated at a lower latitude in a location more exposed to atmospheric transport from lower latitude regions [*Stohl*, 2006]. This may explain why the $\Delta^{17}O$ variability is larger at Barrow, because this location is subjected to large variations in the origin of the air masses, thus leading to highly variable $\Delta^{17}O$ values. This may additionally explain why $\Delta^{17}O$ is generally lower at Barrow than at Alert–and even at La Jolla, California–in our records, especially in winter. Indeed, during this period of the year, local NO_x sources are generally negligible so that most of the nitrate sampled stems from long-range transport, which in the case of Barrow may carry a lower $\Delta^{17}O$ signature owing to a source region featuring different photochemical conditions. Addressing this issue would require a modeling study of $\Delta^{17}O$ of atmospheric nitrate where advection of the relevant variables should explicitly be taken into account, both for the nitrate mass and for its isotopic composition. This would constitute a refinement of the modeling approach by *Alexander et al.* [2009], where the impact of atmospheric transport of nitrate on $\Delta^{17}O$ using the GEOS-Chem global chemistry-transport model was unfortunately not considered.

[33] At Alert, the main origin of the air masses is in the Arctic, thus variations in $\Delta^{17}O$ are much lower, and simply

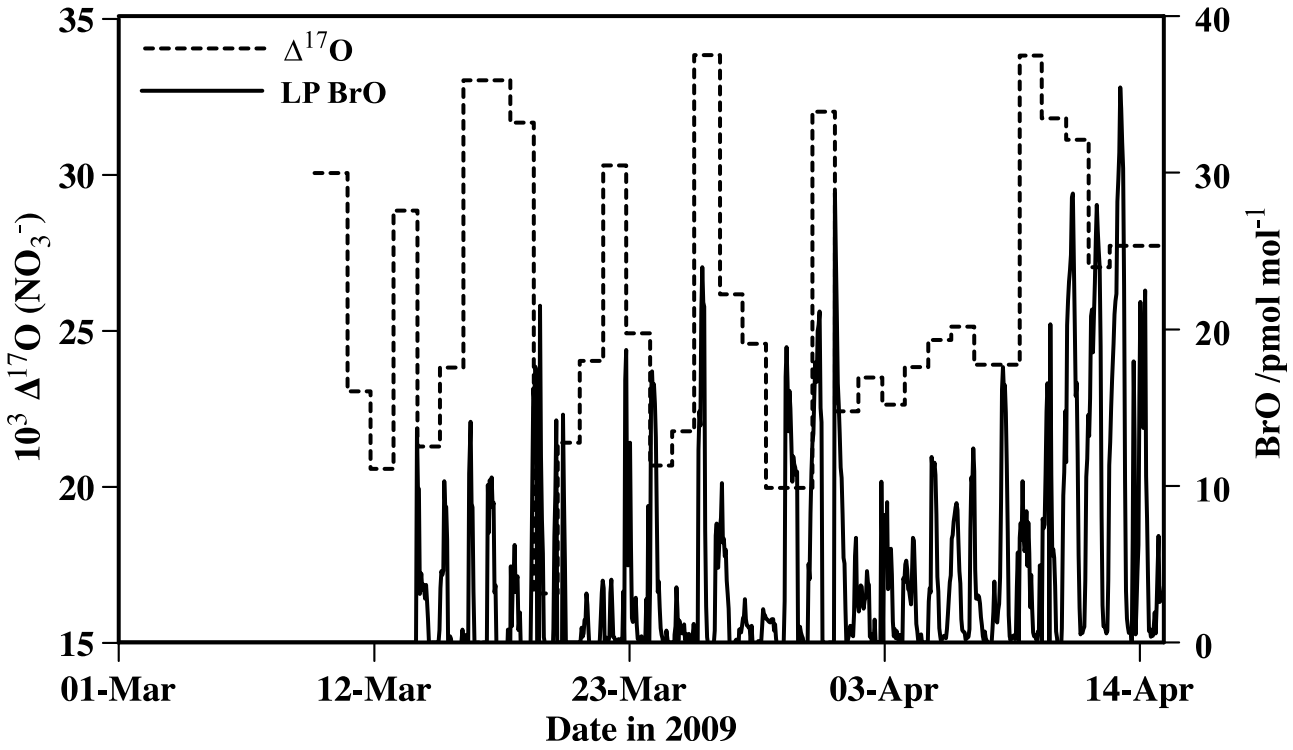

Figure 7. Time series of $\Delta^{17}O$ (dashed line) and the mixing ratio of BrO (solid line) at the surface in March and April 2009 at Barrow, Alaska.

follow the seasonal evolution of the local photochemical activity [*Morin et al.*, 2008]. $\Delta^{17}O$ measurements in mid-latitudes locations such La Jolla [*Michalski et al.*, 2003] and the Cape Verde Observatory (Savarino et al., manuscript in preparation, 2012) also exhibit smooth seasonal variations, due to the fact that the origin of the air masses remains approximately the same throughout the year and thus exhibits smooth seasonal variations in photochemical activity. Note that these considerations have to be placed in the context of the atmospheric lifetime of nitrate, which is on the order of one week [*Finlayson-Pitts and Pitts*, 2000].

[34] The main commonality between the Barrow and the Alert data-set is that highest $\Delta^{17}O$ values are found during springtime, based on single measurements (see Figure 1). The 10-day averaging procedure at Barrow tends to limit the influence of these high-$\Delta^{17}O$ samples, because they feature a lower concentration than the lower-$\Delta^{17}O$ samples. Nevertheless, the presence of the highest $\Delta^{17}O$ values during springtime at Barrow is consistent with previous observations carried out at Alert [*Morin et al.*, 2008].

[35] The presence of reactive halogen radicals such as BrO in the MBL has a profound influence on the oxidative capacity of the atmosphere during Arctic springtime [*Simpson et al.*, 2007, and references therein]. In terms of the chemical budget of NO_x and the isotopic signature of nitrate, the impact of BrO can occur within two chemical mechanisms. First of all, BrO can oxidize NO to form NO_2, thereby superseding NO oxidants such as ozone or HO_2. Since BrO is believed to carry a similar $\Delta^{17}O$ signature as the one transferred by ozone to NO, the isotopic impact of the presence of BrO on $\Delta^{17}O$ of NO_2 only stems from a different ratio between the mixing ratios of NO oxidants [*Morin et al.*, 2007b, 2011]. More germane to the $\Delta^{17}O$ of atmospheric nitrate, it has long been recognized that BrO could react with NO_2 to form $BrONO_2$, the hydrolysis of which is a potentially significant NO_x sink reaction [*Sander et al.*, 1997]:

$$BrONO_2 + H_2O \rightarrow HNO_3 + HOBr \quad (5)$$

In the context of tropospheric ozone depletion, it is worth mentioning that the latter reaction contributes to reactive bromine recycling, since the hydrolysis of $BrONO_2$ on aerosol particles leads to particulate nitrate and HOBr, whose photolysis returns a potent Br radical into the atmosphere, where it can further contribute to ozone destruction [*Simpson et al.*, 2007]. *Morin et al.* [2007b] have shown that the hydrolysis of $BrONO_2$ could lead to the highest possible $\Delta^{17}O$ signature in atmospheric nitrate, in contrast to nitrate produced homogeneously through the $OH + NO_2$ reaction or heterogeneously through the hydrolysis of N_2O_5 [*Morin et al.*, 2009, 2011]. While we do not repeat over the arguments presented in previous publications, we note here that at Barrow and Alert, $\Delta^{17}O$ indeed maximizes during springtime, as evidenced in Figure 3. This is fully consistent with the seasonality of the presence of BrO in the Arctic troposphere as observed using satellite-borne spectroscopy [*Richter et al.*, 2002; *Hollwedel et al.*, 2004; *Friess et al.*, 2011, and references therein]. That the importance of reactive halogen chemistry in the Arctic MBL peaks during springtime is thus substantiated by two independent means (remote-sensing and nitrate isotopic analysis). In lack of a consistent chemistry-transport model fully including reactive halogens and an

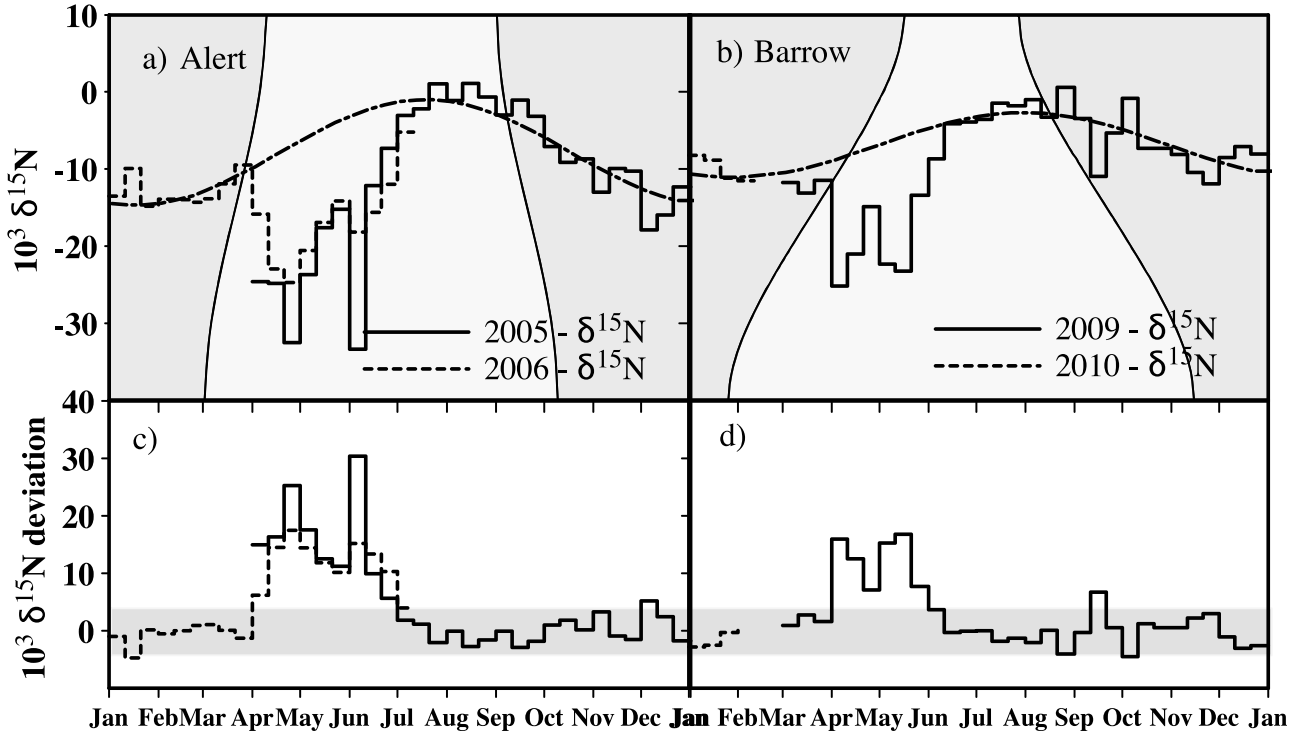

Figure 8. Time series of the seasonal variation of δ^{15}N of atmospheric nitrate at Alert, Nunavut, 82°N [*Morin et al.*, 2008] and Barrow, Alaska, 71°N [this study]. Seasonal variations of δ^{15}N at (a) Alert, Nunavut and (b) Barrow, Alaska, along with the cosine curve resulting from the fitting procedure described in section 2.1 for both sites. The deviation of δ^{15}N from the idealized seasonal variation at (c) Alert and (d) Barrow. Positive deviations indicate a significant contribution of snowpack emissions of NO_x, inducing a low δ^{15}N signature in locally produced atmospheric nitrate. The shaded areas in Figures 8c and 8 d indicate the −5 / +5 ‰ threshold above which deviations are considered significant.

explicit computation of Δ^{17}O of nitrate, the interpretation of the data cannot be further refined at this stage.

4.3. Evidence for Chemical Coupling Between Snowpack NO_x Emissions and Reactive Halogens During Springtime

[36] As shown in section 2.2, we do not find a correlation between the mixing ratio of ozone or BrO and daily Δ^{17}O of atmospheric nitrate values. This is actually not such a surprise given the large differences in the atmospheric lifetime of ozone, BrO and atmospheric nitrate. While ozone has a lifetime which is believed to drop to several hours in the presence of reactive halogens [*Jacobi et al.*, 2006], and that BrO exhibits marked diurnal cycles [*Pöhler et al.*, 2010; *Friess et al.*, 2011], atmospheric nitrate has a much longer lifetime, on the order of one week [*Finlayson-Pitts and Pitts*, 2000]. The interpretation of time variations of Δ^{17}O at the scale of 10-day periods, which exceeds the atmospheric lifetime of nitrate, can thus be carried out considering that the isotopic composition and the concentration of atmospheric nitrate is governed by steady state solutions of the continuity equations [*Michalski et al.*, 2003; *Kunasek et al.*, 2008; *Morin et al.*, 2009, 2011]. This consideration allows to interpret isotopic composition of nitrate directly in terms of the isotopic contribution of its different sources. However, a corollary of this observation is that the interpretation of subdiurnal variations of Δ^{17}O, for instance contrasted with in-situ measurements of trace species such as BrO and ozone, cannot be carried out directly and that only a atmospheric chemistry model can help disentangling issues associated with the various timescales involved [*Morin et al.*, 2011].

[37] Figure 10 shows the day-to-day variation of Δ^{17}O versus that of δ^{15}N. On this plot, most of the data collected during the OASIS intensive field campaign fall in the region where the two variations have opposite signs. Stated simply, it graphically shows that variations of δ^{15}N and Δ^{17}O are anticorrelated. Both the idealized seasonal variations of Δ^{17}O and δ^{15}N are small on a day-to-day basis. The variabilities in δ^{15}N and Δ^{17}O thus have to be attributed to snowpack NO_x emissions and reactive halogen oxidation of NO_x, respectively, which are both potentially intermittent in time and space. The decrease of δ^{15}N over time has to be interpreted as an increase in the contribution of snowpack NO_x to atmospheric NO_x. In this situation, the data indicate that Δ^{17}O increases, which has to be interpreted as an increase in reactive halogen oxidation of NO_x. It thus appears that air masses exposed to injections of NO_x originating from snowpack photodenitrification also undergo extensive reactive halogen chemistry whereby the snowpack-emitted NO_x is oxidized into nitrate. This observation, solely made on the basis of dual isotopic measurements of atmospheric nitrate, reveals a strong coupling between NO_x emissions from the snowpack and reactive halogen chemistry. It confirms

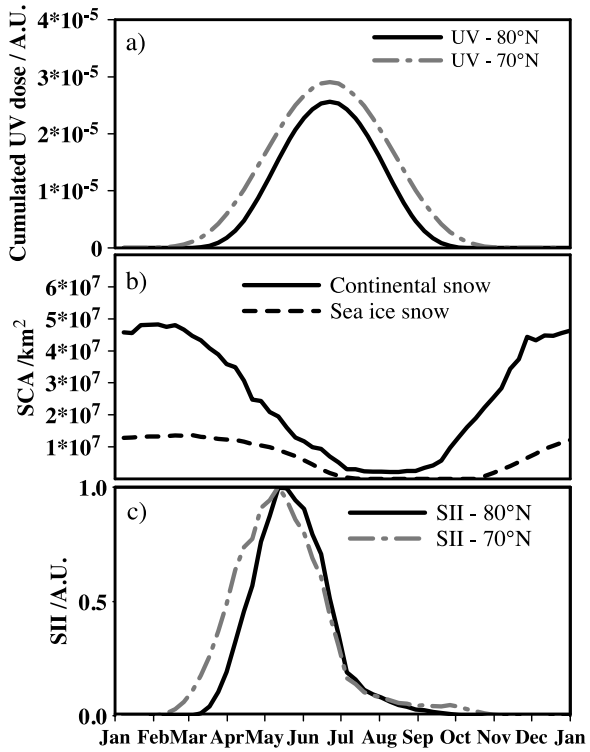

Figure 9. Factors involved in the snow illumination index (SII). (a) Seasonal variation of the daily UV dose at the surface at 70°N and 80°N, corresponding to the latitude of Barrow, Alaska and Alert, Nunavut, respectively; (b) estimate of the seasonal snow covered area in the Arctic, on continents and on sea-ice; and (c) computation of the snow illumination index as the multiplication of the above two curves, for illumination conditions of 70°N and 80°N, respectively. Note that the snow illumination index is dimensionless and ranges between 0 and 1.

previous such assessments carried out on lower-resolution isotopic data sets [*Morin et al.*, 2008, 2009] or on measurement-based box-modeling [*Bauguitte et al.*, 2009].

[38] It is tempting to investigate the nature of the causal link behind the temporal correlation found between snowpack NO_x emissions and reactive halogen chemistry. Common driving factors include the presence of snow and UV light [*Grannas et al.*, 2007; *Friess et al.*, 2011, and references therein]. It could thus simply be that both phenomena are driven by the same external forcing, which would explain the observed correlation. However, links between the photochemistry of nitrate and reactive halogens in the snow have recently been revealed by laboratory experiments. For example, *Richards et al.* [2010] have recently demonstrated that the photolysis of nitrate adsorbed on snow crystals was enhanced in the presence of bromide ions. Conversely, under the hypothesis that acidic conditions are needed for the activation of reactive halogen chemistry on frozen surfaces [*Fan and Jacob*, 1992], the hydrolysis of $BrONO_2$ could provide acidic conditions to surfaces prone to halogen activation. The presence of $BrONO_2$ in the Arctic atmosphere can only be due to local NO_2 emission by the snowpack, in the absence of any other NO_x source [*Morin et al.*, 2008]. These two examples indicate how snowpack NO_x emissions and reactive halogen chemistry can be interrelated, and possibly mutually reinforcing.

5. Summary and Implications

[39] Based on new measurements of the dual isotopic composition ($\Delta^{17}O$ and $\delta^{15}N$) of nitrate from the Arctic atmosphere, obtained at Barrow, Alaska, during the intensive OASIS field campaign in spring 2009 and continued until February 2010 at a weekly time resolution, this paper refines and confirms several hypotheses which were exposed in previous publications [*Morin et al.*, 2008, 2009], regarding the cycling of reactive nitrogen in the Arctic atmosphere:

[40] 1. The seasonal variations of $\delta^{15}N$ in atmospheric nitrate in the Arctic can be considered as the result of the superposition of two processes: one -yet to be identified- process drives yearly variations of $\delta^{15}N$ showing a maximum around 0 ‰ in summer and a minimum around −10 ‰ in winter. The average $\delta^{15}N$ values in the Arctic are generally more negative and span a wider range than at midlatitudes and tropical sites. During springtime, $\delta^{15}N$ is dominated by the relative importance of nitrate production from NO_x emitted through the photodenitrification of the snowpack. Indeed, this source possesses a peculiar low $\delta^{15}N$ signature, which can lead to $\delta^{15}N$ values in atmospheric nitrate down to −40 ‰ in springtime. A secondary maximum in snowpack emissions was found, for the first time, in $\delta^{15}N$ data from Barrow, Alaska, in September. At first order, the seasonality of snowpack NO_x emissions is explained by the combination of UV availability at the surface and the snow area with which UV can interact at the regional scale.

[41] 2. At the daily time-scale, our measurements reveal a significant interplay between NO_x emissions by the snowpack,

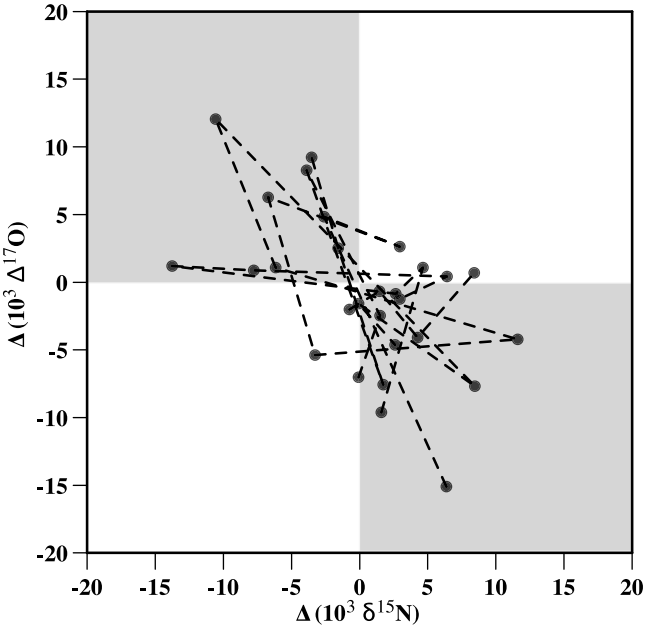

Figure 10. Sample-to-sample variation of $\Delta^{17}O$ versus that of $\delta^{15}N$ during the intensive OASIS 2009 campaign (March–April 2009, Barrow, Alaska), when the sampling rate was approximately daily. Dashed lines link consecutive measurements.

and its subsequent oxidation by reactive halogens. Indeed, as noted before based on a much more limited data-set, reactive halogen oxidation of NO_x (mainly in the form of $BrONO_2$) can only proceed if NO_x are locally emitted by the snowpack. Long-range transport of NO_x to the Arctic is insignificant [*Morin et al.*, 2008], so that emissions of NO_x from the snowpack are the only possible local source of NO_x in the Arctic atmosphere at present, until anthropogenic emissions of NO_x start playing a significant role [*Granier et al.*, 2006]. The evidence for this coupling confirms and strengthens model conclusions constrained by measurements of mixing ratios of atmospheric NO_x and other trace gases [*Bauguitte et al.*, 2009; *Moller et al.*, 2010] in a totally independent way. Measurements of the isotope anomaly of NO_2, in the atmosphere or within the snowpack, would help deciphering further this interplay.

[42] 3. Dual isotopic measurements of atmospheric nitrate have proven useful to infer the presence of snow photodenitrification in polar environments. Compared to flux or reactive trace gases direct measurements, atmospheric nitrate measurements are extremely easy and little demanding to implement within a suite of atmospheric chemistry measurements, and could potentially be routinely carried out for future intensive or monitoring atmospheric chemistry studies. Recent studies have shown how such variables can be implemented in atmospheric chemistry box models [*Gromov et al.*, 2010; *Morin et al.*, 2011] or in larger chemistry-transport models [*Alexander et al.*, 2009]. Due to the large variations in the life time of species involved in NO_x-halogen chemical interplay, only numerical modeling along with air mass trajectories will shed light on the detailed chemical processes affecting the isotopic composition of atmospheric nitrate, hence providing the tools to interpret more quantitatively the variations observed.

[43] 4. Photodenitrification of the snowpack seems to be a general feature found everywhere it is investigated [*Grannas et al.*, 2007; *Morin et al.*, 2008; *Frey et al.*, 2009; *Bauguitte et al.*, 2009; *Moller et al.*, 2010]. Due to its impact on the isotopic composition and concentration of nitrate remaining in the snow, it has to be taken into account when attempting to derive chemical information on the budget of atmospheric reactive nitrogen from firn or ice core records of nitrate concentration and isotopic composition.

[44] **Acknowledgments.** We thank Patricia K. Quinn (NOAA PMEL, Seattle WA, USA) for helping organizing the sampling at the NOAA Observatory, as well as Dan Endres, Steve Grove, Jason Johns and Matthew Martinsen for aerosol sampling at the NOAA Observatory, under the auspices of the NOAA-ESRL Cooperative Research Project GMD-2009-01-QUINN. INSU LEFE is acknowledged for funding through project "LICENCE." The French Polar Institute (IPEV) is acknowledged for partly funding the French contribution to OASIS 2009. We thank Envirhonalp for its support through the plateau MOME, Erwann Vince for bacterial cultures at LTHE, Jean-Luc Jaffrezo and Julie Cozic for chemical analyses at LGGE and W. C. Vicars for help with isotopic measurements. Positive and encouraging reviews by Becky Alexander (Univ. Washington, Seattle WA, USA) and one anonymous reviewer are acknowledged.

References

Alexander, B., M. G. Hastings, D. J. Allman, J. Dachs, J. A. Thornton, and S. A. Kunasek (2009), Quantifying atmospheric nitrate formation pathways based on a global model of the oxygen isotopic composition ($\Delta^{17}O$) of atmospheric nitrate, *Atmos. Chem. Phys.*, *9*, 5043–5056, doi:10.5194/acp-9-5043-2009.

Amoroso, A., et al. (2010), Microorganisms in dry polar snow are involved in the exchanges of reactive nitrogen species with the atmosphere, *Environ. Sci. Technol.*, *44*(2), 714–719, doi:10.1021/es9027309.

Barrie, L. A., J. W. Bottenheim, R. A. Rasmussen, R. C. Schnell, and P. J. Crutzen (1988), Ozone destruction and photochemical reactions at polar sunrise in the lower Arctic troposphere, *Nature*, *334*, 138–141.

Bauguitte, S. J.-B., et al. (2009), Summertime NO_x measurements during the CHABLIS campaign: Can source and sink estimates unravel observed diurnal cycles?, *Atmos. Chem. Phys. Discuss.*, *9*, 20,371–20,406.

Blunier, T., G. L. Floch, H.-W. Jacobi, and E. Quansah (2005), Isotopic view on nitrate loss in Antarctic surface snow, *Geophys. Res. Lett.*, *32*, L13501, doi:10.1029/2005GL023011.

Böhlke, J. K., S. J. Mroczkowski, and T. B. Coplen (2003), Oxygen isotopes in nitrate: new reference materials for ^{18}O:^{17}O:^{16}O measurements and observations on nitrate-water equilibration, *Rapid Commun. Mass Spectrom.*, *17*, 1835–1846.

Bottenheim, J. W., A. J. Gallant, and K. A. Brice (1986), Measurements of NO_y species and O_3 at 82°N latitude, *Geophys. Res. Lett.*, *13*, 113–116.

Bottenheim, J. W., S. Netcheva, S. Morin, and S. V. Nghiem (2009), Ozone in the boundary layer air over the Arctic Ocean: Measurements during the TARA transpolar drift 2006–2008, *Atmos. Chem. Phys.*, *9*, 4545–4557.

Boxe, C. S., and A. Saiz-Lopez (2008), Multiphase modeling of nitrate photochemistry in the quasi-liquid layer (QLL): Implications for NO_x release from the Arctic and coastal Antarctic snowpack, *Atmos. Chem. Phys.*, *8*, 4855–4864.

Brenninkmeijer, C. A. M., C. Janssen, J. Kaiser, T. Röckmann, T. S. Rhee, and S. S. Assonov (2003), Isotope effects in the chemistry of atmospheric trace compounds, *Chem. Rev.*, *103*(12), 5125–5162, doi:10.1021/cr020644k.

Calvert, J. G., and S. Lindberg (2003), A modeling study of the mechanism of the halogen/ozone/mercury homogeneous reactions in the troposphere during the polar spring, *Atmos. Environ.*, *37*, 4467–4481, doi:10.1016/j.atmosenv.2003.07.001.

Casciotti, K. L., D. M. Sigman, M. G. Hastings, J. K. Böhlke, and A. Hilkert (2002), Measurement of the oxygen isotopic composition of nitrate in seawater and freshwater using the denitrifier method, *Anal. Chem.*, *74*, 4905–4912, doi:10.1021/ac020113w.

Crawford, J. H., et al. (2001), Evidence for photochemical production of ozone at the South Pole surface, *Geophys. Res. Lett.*, *28*(19), 3641–3644.

Dominé, F., and P. B. Shepson (2002), Air-snow interactions and atmospheric chemistry, *Science*, *297*, 1506–1510.

Dommergue, A., F. Sprovieri, N. Pirrone, R. Ebinghaus, S. Brooks, J. Courteaud, and C. P. Ferrari (2010), Overview of mercury measurements in the Antarctic troposphere, *Atmos. Chem. Phys.*, *10*, 3309–3319.

Drobot, S. D., and M. R. Anderson (2001), An improved method for determining snowmelt onset dates over Arctic sea ice using scanning multichannel microwave radiometer and Special Sensor Microwave/Imager data, *J. Geophys. Res.*, *106*, 24,033–24,049.

Evans, M. J., et al. (2003), Coupled evolution of BrO_x-ClO_x-HO_x-NO_x chemistry during bromine-catalyzed ozone depletion events in the arctic boundary layer, *J. Geophys. Res.*, *108*(D4), 8368, doi:10.1029/2002JD002732.

Fan, S. M., and D. J. Jacob (1992), Surface ozone depletion in Arctic spring sustained by bromine reactions on aerosols, *Nature*, *359*, 522–524, doi:10.1038/359522a0.

Finlayson-Pitts, B. J., and J. N. Pitts (2000), *Chemistry of the Upper and Lower Atmosphere: Theory, Experiments and Applications*, Academic, San Diego, Calif.

Frey, M. M., J. Savarino, S. Morin, J. Erbland, and J. M. F. Martins (2009), Photolytic imprint in the nitrate stable isotope signal in snow and atmosphere of East Antarctica and implications for reactive nitrogen cycling, *Atmos. Chem. Phys.*, *9*, 8681–8696, doi:10.5194/acp-9-8681-2009.

Freyer, H. D. (1991), Seasonal variation of $^{15}N/^{14}N$ ratios in atmospheric nitrate species, *Tellus, Ser. B*, *43*, 30–44.

Freyer, H. D., D. Kley, A. Volz-Thomas, and K. Kobel (1993), On the interaction of isotopic exchange processes with photochemical reactions in atmospheric oxides of nitrogen, *J. Geophys. Res.*, *98*(D8), 14,791–14,796.

Freyer, H. D., K. Kobel, R. J. Delmas, D. Kley, and M. R. Legrand (1996), First results of $^{15}N/^{14}N$ ratios in nitrate from alpine and polar ice cores, *Tellus, Ser. B*, *48*(1), 93–105.

Friess, U., H. Sihler, R. Sander, D. Pöhler, S. Yilmaz, and U. Platt (2011), The vertical distribution of BrO and Aerosols in the Arctic: Measurements by active and passive DOAS, *J. Geophys. Res.*, *116*, D00R04, doi:10.1029/2011JD015938.

Granier, C., U. Niemeier, J. H. Jungclaus, L. Emmons, P. Hess, J.-F. Lamarque, S. Walters, and G. P. Brasseur (2006), Ozone pollution from future ship traffic in the arctic northern passages, *Geophys. Res. Lett.*, *33*, L13807, doi:10.1029/2006GL026180.

Grannas, A. M., et al. (2007), An overview of snow photochemistry: evidence, mechanisms and impacts, *Atmos. Chem. Phys.*, *7*, 4329–4373.

Gromov, S., P. Jöckel, R. Sander, and C. A. M. Brenninkmeijer (2010), A kinetic chemistry tagging technique and its application to modelling the stable isotopic composition of atmospheric trace gases, *Geosci. Model Dev.*, *3*, 337–364, doi:10.5194/gmd-3-337-2010.

Hastings, M. G., E. J. Steig, and D. M. Sigman (2004), Seasonal variations in N and O isotopes of nitrate in snow at Summit, Greenland: Implications for the study of nitrate in snow and ice cores, *J. Geophys. Res.*, *109*, D20306, doi:10.1029/2004JD004991.

Hausmann, M., and U. Platt (1994), Spectroscopic measurement of bromine oxide and ozone in the high Arctic during Polar Sunrise Experiment 1992, *J. Geophys. Res.*, *99*(D12), 25,399–25,413.

Helmig, D., S. J. Oltmans, T. O. Morse, and J. E. Dibb (2007), What is causing high ozone at Summit, Greenland?, *Atmos. Environ.*, *41*(24), 5031–5043, doi:10.1016/j.atmosenv.2006.05.084.

Hollwedel, J., M. Wenig, S. Beirle, S. Kraus, S. Kühl, W. Wilms-Grabe, U. Platt, and T. Wagner (2004), Year-to-year variations of spring time polar tropospheric BrO as seen by GOME, *Adv. Space Res.*, *34*, 804–808, doi:10.1016/j.asr.2003.08.060.

Honrath, R. E., M. C. Peterson, S. Guo, J. E. Dibb, P. B. Shepson, and B. Campbell (1999), Evidence of NO_x production within or upon ice particles in the Greenland snowpack, *Geophys. Res. Lett.*, *26*(6), 695–698.

Jacobi, H. W., L. Kaleschke, A. Richter, A. Rozanov, and J. P. Burrows (2006), Observation of fast ozone loss over frost flowers in the marginal ice zone of the Arctic Ocean, *J. Geophys. Res.*, *111*, D15309, doi:10.1029/2005JD006715.

Jarvis, J. C., E. J. Steig, M. G. Hastings, and S. A. Kunasek (2008), Influence of local photochemistry on isotopes of nitrate in Greenland snow, *Geophys. Res. Lett.*, *35*, L21804, doi:10.1029/2008GL035551.

Kaiser, J., T. Röckmann, and C. A. M. Brenninkmeijer (2004), Contribution of mass-dependent fractionation to the oxygen isotope anomaly of atmospheric nitrous oxide, *J. Geophys. Res.*, *109*, D03305, doi:10.1029/2003JD004088.

Kaiser, J., M. G. Hastings, B. Z. Houlton, T. Röckmann, and D. M. Sigman (2007), Triple oxygen isotope analysis of nitrate using the denitrifier method and thermal decomposition of N_2O, *Anal. Chem.*, *79*(2), 599–607, doi:10.1021/ac061022s.

Kendall, C., E. M. Elliott, and S. D. Wankel (2007), Tracing anthropogenic inputs of nitrogen to ecosystems, in *Stable Isotopes in Ecology and Environmental Science*, 2nd ed., chap. 12, pp. 375–449, Blackwell, Malden, Mass.

Kunasek, S. A., B. Alexander, E. J. Steig, M. G. Hastings, D. J. Gleason, and J. C. Jarvis (2008), Measurements and modeling of $\Delta^{17}O$ of nitrate in snowpits from Summit, Greenland, *J. Geophys. Res.*, *113*, D24302, doi:10.1029/2008JD010103.

Legrand, M., S. Preunkert, B. Jourdain, H. Gallée, F. Goutail, R. Weller, and J. Savarino (2009), Year-round record of surface ozone at coastal (Dumont d'Urville) and inland (Concordia) sites in East Antarctica, *J. Geophys. Res.*, *114*, D20306, doi:10.1029/2008JD011667.

Liao, J., et al. (2011), A comparison of Arctic BrO measurements by chemical ionization mass spectrometry and long path-differential optical absorption spectroscopy, *J. Geophys. Res.*, *116*, D00R02, doi:10.1029/2010JD014788.

Lu, J. Y., W. H. Schroeder, L. A. Barrie, A. Steffen, H. E. Welch, K. Martin, L. Lockhart, R. V. Hunt, G. Boila, and A. Richter (2001), Magnification of atmospheric mercury deposition to polar regions in springtime: The link to tropospheric ozone depletion chemistry, *Geophys. Res. Lett.*, *28*(17), 3219–3222.

Marcus, R. A. (2008), Mass-independent oxygen isotope fractionation in selected systems. Mechanistic considerations, *Adv. Quantum Chem.*, *55*, 5–19, doi:10.1016/S0065-3276(07)00202-X.

Michalski, G., Z. Scott, M. Kabiling, and M. H. Thiemens (2003), First measurements and modeling of $\Delta^{17}O$ in atmospheric nitrate, *Geophys. Res. Lett.*, *30*(16), 1870, doi:10.1029/2003GL017015.

Moller, S. J., et al. (2010), Measurements of nitrogen oxides from Hudson Bay: Implications for NO_x release from snow and ice covered surfaces, *Atmos. Environ.*, *44*(25), 2971–2979, doi:10.1016/j.atmosenv.2010.05.015.

Morin, S., J. Savarino, S. Bekki, A. E. Cavender, P. B. Shepson, and J. W. Bottenheim (2007a), Major influence of BrO on the NO_x budget in the Arctic spring, inferred from $\Delta^{17}O(NO_3^-)$ measurements during ozone depletion events, *Environ. Chem.*, *4*, 238–241, doi:10.1071/EN07003.

Morin, S., J. Savarino, S. Bekki, S. Gong, and J. W. Bottenheim (2007b), Signature of Arctic surface ozone depletion events in the isotope anomaly ($\Delta^{17}O$) of atmospheric nitrate, *Atmos. Chem. Phys.*, *7*, 1451–1469, doi:10.5194/acp-7-1451-2007.

Morin, S., J. Savarino, M. M. Frey, N. Yan, S. Bekki, J. W. Bottenheim, and J. M. F. Martins (2008), Tracing the origin and fate of NO_x in the Arctic atmosphere using stable isotopes in nitrate, *Science*, *322*, 730–732, doi:10.1126/science.1161910.

Morin, S., J. Savarino, M. M. Frey, F. Domine, H. W. Jacobi, L. Kaleschke, and J. M. F. Martins (2009), Comprehensive isotopic composition of atmospheric nitrate in the Atlantic Ocean boundary layer from 65°S to 79°N, *J. Geophys. Res.*, *114*, D05303, doi:10.1029/2008JD010696.

Morin, S., R. Sander, and J. Savarino (2011), Simulation of the diurnal variations of the oxygen isotope anomaly ($\Delta^{17}O$) of reactive atmospheric species, *Atmos. Chem. Phys.*, *11*, 3653–3671, doi:10.5194/acp-11-3653-2011.

Patey, M. D., M. J. A. Rijkenberg, P. J. Statham, M. C. Stinchcombe, E. P. Achterberg, and M. Mowlem (2008), Determination of nitrate and phosphate in seawater at nanomolar concentrations, *Trends Anal. Chem.*, *27*(2), 169–182, doi:10.1016/j.trac.2007.12.006.

Pöhler, D., L. Vogel, U. Friess, and U. Platt (2010), Observation of halogen species in the Amundsen Gulf, Arctic, by active long-path differential optical absorption spectroscopy, *Proc. Natl. Acad. Sci. U. S. A.*, *107*(15), 6582—6587, doi:10.1073/pnas.0912231107.

Quinn, P. K., G. Shaw, E. Andrew, E. G. Dutton, T. Ruoho-Airola, and S. L. Gong (2007), Arctic haze: Current trends and knowledge gaps, *Tellus, Ser. B*, *59*, 99–114, doi:10.1111/j.1600-0889.2006.00238.x.

Richards, N. K., L. M. Wingen, K. M. Callahan, N. Nishino, M. T. Kleinman, D. J. Tobias, and B. J. Finlayson-Pitts (2010), Nitrate ion photolysis in thin water films in the presence of bromide ions, *J. Phys. Chem. A*, *115*(23), 5810–-5821, doi:10.1021/jp109560j.

Richter, A., F. Wittrock, A. Ladstätter-Weissenmayer, and J. P. Burrows (2002), GOME measurements of stratospheric and tropospheric BrO, *Adv. Space Res.*, *29*(11), 1667–1672.

Robinson, D. A., and A. Frei (2000), Variability of northern hemisphere snow extent using visible satellite data, *Prof. Geogr.*, *51*, 307–314.

Saiz-Lopez, A., A. S. Mahajan, R. A. Salmon, S. J.-B. Bauguitte, A. E. Jones, H. K. Roscoe, and J. M. C. Plane (2007), Boundary layer halogens in coastal Antarctica, *Science*, *317*, 348–351, doi:10.1126/science.1141408.

Sander, R., R. Vogt, G. Harris, and P. Crutzen (1997), Modeling the chemistry of ozone, halogen compounds, and hydrocarbons in the arctic troposphere during spring, *Tellus, Ser. B*, *49*, 522–532.

Sander, R., Y. Rudich, R. von Glasow, and P. J. Crutzen (1999), The role of $BrNO_3$ in marine tropospheric chemistry: A model study, *Geophys. Res. Lett.*, *26*, 2857–2860.

Savarino, J., and S. Morin (2011), The N, O, S isotopes of oxy-anions in ice cores and polar environments, in *Handbook of Environmental Isotope Geochemistry*, chap. 39, pp. 835–864, Springer, New York, doi:10.1007/978-3-642-10637-8_39.

Savarino, J., J. Kaiser, S. Morin, D. M. Sigman, and M. H. Thiemens (2007), Nitrogen and oxygen isotopic constraints on the origin of atmospheric nitrate in coastal Antarctica, *Atmos. Chem. Phys.*, *7*, 1925– 1945, doi:10.5194/acp-7-1925-2007.

Schroeder, W. H., K. Anlauf, L. A. Barrie, J. Y. Lu, A. Steffen, D. R. Schneeberger, and T. Berg (1998), Arctic springtime depletion of mercury, *Nature*, *394*, 331–332.

Sigman, D. M., K. L. Casciotti, M. Andreani, C. Barford, M. Galanter, and J. K. Böhlke (2001), A bacterial method for the nitrogen isotopic analysis of nitrate in marine and fresh waters, *Anal. Chem.*, *73*, 4145–4153.

Simpson, W. R., et al. (2007), Halogens and their role in polar boundary-layer ozone depletion, *Atmos. Chem. Phys.*, *7*, 4375–4418.

Sirois, A., and L. A. Barrie (1999), Arctic lower tropospheric aerosol trends and composition at Alert, Canada: 1980–1995, *J. Geophys. Res.*, *104*, 11,599–11,618.

Snape, C. E., C. Sun, A. E. Fallick, R. Irons, and J. Haskell (2003), Potential of stable nitrogen isotope ratio measurements to resolve fuel and thermal NO_x in coal combustion, *Prepr. Pap. Am. Chem. Soc. Div. Fuel Chem.*, *48*(1), 3–5.

Steffen, A., et al. (2008), A synthesis of atmospheric mercury depletion event chemistry in the atmosphere and snow, *Atmos. Chem. Phys.*, *8*, 1445–1482.

Stohl, A. (2006), Characteristics of atmospheric transport into the Arctic troposphere, *J. Geophys. Res.*, *111*, D11306, doi:10.1029/2005JD006888.

Sumner, A. L., and P. B. Shepson (1999), Snowpack production of formaldehyde and its effect on the Arctic troposphere, *Nature*, *398*, 230–233.

Thiemens, M. H. (2006), History and applications of mass-independent isotope effects, *Annu. Rev. Earth Planet. Sci.*, *34*, 217–262, doi:10.1146/annurev.earth.34.031405.125026.

Wagenbach, D., M. Legrand, H. Fischer, F. Pichlmayer, and E. W. Wolff (1998), Atmospheric near-surface nitrate at coastal Antarctic sites, *J. Geophys. Res.*, *103*(D9), 11,007–11,020.

Wankel, S. D., Y. Chen, C. Kendall, A. F. Post, and A. Paytan (2010), Sources of aerosol nitrate to the Gulf of Aqaba: Evidence from $\delta^{15}N$ and $\delta^{18}O$ of nitrate and trace metal chemistry, *Mar. Chem.*, *120*(1–4), 90–99, doi:10.1016/j.marchem.2009.01.013.

Zhou, X., H. J. Beine, R. E. Honrath, J. D. Fuentes, W. Simpson, P. B. Shepson, and J. W. Bottenheim (2001), Snowpack photochemical

production of HONO: A major source of OH in the Arctic boundary layer in springtime, *Geophys. Res. Lett.*, *28*(21), 4087–4090.

J. Bock, J. Erbland, H.-W. Jacobi, and J. Savarino, LGGE, 54 rue Molière, F-38400 St. Martin d'Hères, France.

F. Domine, Département de Biologie/Pavillon Alexandre-Vachon, Université Laval, 1045 av. de la Médecine, Québec, QC G1V 0A6, Canada.

U. Friess and H. Sihler, Institut für Umweltphysik, Universität Heidelberg, Im Neuenheimer Feld 229, D-69120 Heidelberg, Germany.

J. M. F. Martins, LTHE, CERMO, 460 rue de la Piscine, F-38400 St. Martin d'Hères, France.

S. Morin, Météo-France/CEN, 1441 rue de la Piscine, F-38400 St. Martin d'Hères, France. (samuel.morin@meteo.fr).